

Supporting Information to Accompany the Communication Entitled:

**Homogeneity of Phytochrome Cph1 Vibronic Absorption Revealed by Resonance Raman Intensity Analysis**

Katelyn M. Spillane,<sup>†</sup> Jyotishman Dasgupta,<sup>†</sup> J. Clark Lagarias,<sup>‡</sup> and Richard A. Mathies<sup>†,\*</sup>

<sup>†</sup>*Department of Chemistry, University of California, Berkeley, California 94720, and*  
<sup>‡</sup>*Department of Molecular and Cellular Biology, University of California, Davis, California 95616*

E-mail: ramathies@berkeley.edu

**Table of Contents**

<b>S1.</b> Experimental Section .....	S-2
<b>S2.</b> Computational Details .....	S-3
<b>S3.</b> Figures and Tables .....	S-7
<b>S4.</b> References .....	S-11

## S1. Experimental Section

The stimulated Raman spectra were obtained using the FSRS setup which has been described previously in detail.<sup>1</sup> Briefly, a home-built mode-locked Ti:sapphire oscillator was amplified by a 1 kHz, 800  $\mu\text{J}$  regenerative amplifier (BMI Alpha 1000/US). This produced a train of 50 fs pulses centered at 795 nm which was used to generate the two pulses necessary for the experiment. The 4 ps narrow bandwidth Raman pump pulse (790.4 nm, 3  $\mu\text{J}$ ) was generated by a grating based pulse stretcher. The Raman probe pulse ( $\sim 20$  fs, 12 nJ) was produced by using a portion of the fundamental for continuum generation in a 3-mm-thick sapphire plate. The non-collinear beams were focused at the sample point. The Raman pump beam was attenuated with an 830 nm long-pass filter, and Raman spectra were measured using the 816–940 nm portions of the probe beam. The beams were dispersed by the spectrograph (ISA HR320) with a 600 grooves/mm grating and then imaged onto a Pixis:100F charge coupled device (CCD, Princeton Instruments). The CCD consists of a  $1340 \times 100$  imaging array of  $20 \times 20 \mu\text{m}$  pixels. The CCD read-out rate is 1 kHz, allowing for single-shot detection. The frequency resolution was  $\sim 10 \text{ cm}^{-1}$ , as determined from the  $802 \text{ cm}^{-1}$  cyclohexane peak.

Prior to spectroscopic studies, samples were dialyzed against 1 L buffer (25 mM TES-KOH, pH 8.0, 25 mM KCl, 10% glycerol) and then concentrated to 10.6  $\text{OD}_{660}/\text{cm}$ . For absolute Raman cross-section calibration, a standard solution of  $\text{NaNO}_3$  (250 mM) in TES-glycerol buffer was used. Samples were flowed through a homemade  $1 \times 2 \times 40$  mm Borofloat-glass flow channel at a rate of  $\sim 1 \text{ mL min}^{-1}$  and measurements were taken at room temperature. The photo-excited material was converted back to the  $P_r$  ground state by irradiation of the 500  $\mu\text{L}$  reservoir by a high-powered LED (720 nm, 5 mW,  $30^\circ$  viewing angle, Roithner Lasertechnik) through an

RG695 long-pass filter. Sample integrity was confirmed by UV/Vis spectroscopy both before and after the experiments.

## S2. Computational Details

Absolute Raman cross-sections of Cph1 were determined as described previously.<sup>2</sup> Briefly, the integrated peak areas were compared to that of an external standard band (the 1045 cm<sup>-1</sup> symmetric stretch of NO<sub>3</sub><sup>-</sup>,  $\partial\sigma_{std}/\partial\Omega = 10.9 \times 10^{-14} \text{ \AA}^2/\text{molecule/steradian}$  at 514.5 nm excitation).<sup>3</sup> The differential cross-section at 514.5 nm was extrapolated to  $1.55 \times 10^{-13} \text{ \AA}^2$  at 790.4 nm, assuming that the scattering cross-section is proportional to  $\nu_S^3\nu_L$ , where  $\nu_S$  and  $\nu_L$  are the frequencies of scattered and laser light, respectively. The differential cross-section of NO<sub>3</sub><sup>-</sup> was then used to calculate the differential cross-section of the 1049 cm<sup>-1</sup> C–OH stretch band of glycerol (in TES buffer) using Equation 1:

$$\left(\frac{\partial\sigma}{\partial\Omega}\right)_{glyc} = \frac{(\nu_S)_{glyc}^3 A_{glyc} c_{std}}{(\nu_S)_{std}^3 A_{std} c_{glyc}} \left(\frac{\partial\sigma}{\partial\Omega}\right)_{std} \quad (1)$$

where  $(\nu_S)_{glyc}$  and  $(\nu_S)_{std}$  are the scattering frequencies,  $A_{glyc}$  and  $A_{std}$  are the integrated peak areas, and  $c_{glyc}$  and  $c_{std}$  are the concentrations of glycerol and NO<sub>3</sub><sup>-</sup>, respectively.

By the same method, the differential cross-sections of Cph1 were calculated using the 1049 cm<sup>-1</sup> glycerol mode as an internal standard. The absolute Raman cross-sections were then determined from Equation 2:

$$\sigma_{Cph1} = \frac{8\pi}{3} \frac{(1+2\rho)}{(1+\rho)} \left(\frac{\partial\sigma}{\partial\Omega}\right)_{Cph1} \quad (2)$$

where the depolarization ratios,  $\rho$ , for all bands of Cph1 were measured and found to be 1/3. Glycerol was used in place of nitrate as the internal standard because inclusion of 250 mM  $\text{NO}_3^-$  would denature the protein. As a result, Raman spectra of solutions of  $\text{NO}_3^-$  in TES-glycerol buffer, and Cph1 in TES-glycerol buffer, were measured separately.

Raman excitation profiles (REPs) were calculated using the time-dependent wavepacket formalism of resonance Raman scattering.<sup>4</sup> The absorption cross-sections,  $\sigma_A$ , were determined by the Fourier transform of  $\langle i|i(t)\rangle$ , where  $|i\rangle$  is the initial vibrational eigenstate on the ground electronic surface and  $|i(t)\rangle$  is the vibrational wavefunction of the initial state propagating on the excited electronic surface (Equation 3). The Raman cross-sections,  $\sigma_R$ , were determined by the square of the half-Fourier transform of  $\langle f|i(t)\rangle$ , where  $|f\rangle$  is the final vibrational eigenstate on the ground electronic surface (Equation 4):

$$\sigma_A = \frac{8\pi E_L e^2 M^2}{6\hbar^2 c n(\theta \sqrt{2\pi})} \int_0^\infty dE \times \exp\left[\frac{-(E - E_0)^2}{2\theta^2}\right] \text{Re} \int_0^\infty dt \langle i|i(t)\rangle e^{-\Gamma_G^2 t^2/\hbar^2} e^{i(E_L + \varepsilon_i)t/\hbar} \quad (3)$$

$$\sigma_R = \frac{8\pi E_S^3 E_L e^4 M^4}{9\hbar^6 c^4 (\theta \sqrt{2\pi})} \int_0^\infty dE \times \exp\left[\frac{-(E - E_0)^2}{2\theta^2}\right] \left| \int_0^\infty dt \langle f|i(t)\rangle e^{-\Gamma_G^2 t^2/\hbar^2} e^{i(E_L + \varepsilon_i)t/\hbar} \right|^2 \quad (4)$$

where  $E_L$  and  $E_S$  refer to the frequencies of the laser and scattered light,  $M$  is the electronic transition length,  $E_0$  is the zero-zero energy,  $\varepsilon_i$  is the vibrational energy of eigenstate  $i$ ,  $\Gamma_G$  is the Gaussian homogeneous broadening, and  $\theta$  is the inhomogeneous broadening.

The time-dependent overlaps,  $\langle i|i(t)\rangle$  and  $\langle f|i(t)\rangle$ , depend on the dimensionless parameter  $\Delta$ , which is the displacement between the ground and excited electronic state harmonic minima.

Raman intensity calculations were performed using the program RRModel.f, which was provided by Anne Myers Kelley from UC Merced, to model the experimental absorption spectra and Raman cross-sections. Relative delta values were initially estimated from the intensities of the observed vibrational bands assuming  $I \propto \omega^2 \Delta^2$ .<sup>5</sup> The overall scaling of  $\Delta$ , homogeneous broadening  $\Gamma_G$ , inhomogeneous broadening  $\theta$ , zero-zero energy  $E_0$ , and electronic transition length  $M$  were then adjusted to provide the best fits.

Absorption Franck-Condon factors were calculated for the 0–0, 0–1, and 0–2 vibronic transitions of modes with  $\Delta > 0.2$ . The products of these one-dimensional overlaps are given in Equations 5–7:<sup>2</sup>

$$\langle 0|m\rangle\langle m|0\rangle = |\langle m|0\rangle|^2 = (s^m/ml)e^{-s} \quad (5)$$

$$\langle 1|m\rangle\langle m|0\rangle = (\Delta/2^{1/2})[\langle 0|m\rangle\langle m|0\rangle - \langle 0|m-1\rangle\langle m-1|0\rangle] \quad (6)$$

$$\langle 2|m\rangle\langle m|0\rangle = 2^{-1/2} \left[ s - 2m + \frac{m^2}{s} \langle 0|m\rangle\langle m|0\rangle - \langle 0|m-1\rangle\langle m-1|0\rangle \right] \quad (7)$$

where  $m$  are the vibrational levels of the excited electronic state and  $s = \Delta^2/2$ . Representative FC overlaps for the 1630  $\text{cm}^{-1}$  mode are shown in Figure S2. The overlaps presented in Figure 1 of the main manuscript include a homogeneous broadening of 10  $\text{cm}^{-1}$ .

Vibronic absorption spectra of  $P_r$  were measured over the temperature range of 281 to 313 K and revealed an isosbestic point at 600 nm (see Figure S3.A). These spectra were simulated using the vibrational frequencies and delta values given in Table 1, and are in excellent agreement with the experimental spectra (see Figure S3.B). For all spectra, the 0–0 transition

energy was  $14800\text{ cm}^{-1}$  and the inhomogeneous broadening was  $90\text{ cm}^{-1}$ . The homogeneous broadening and electronic transition length parameters used in the calculations are given in Table S1.

### S3. Figures

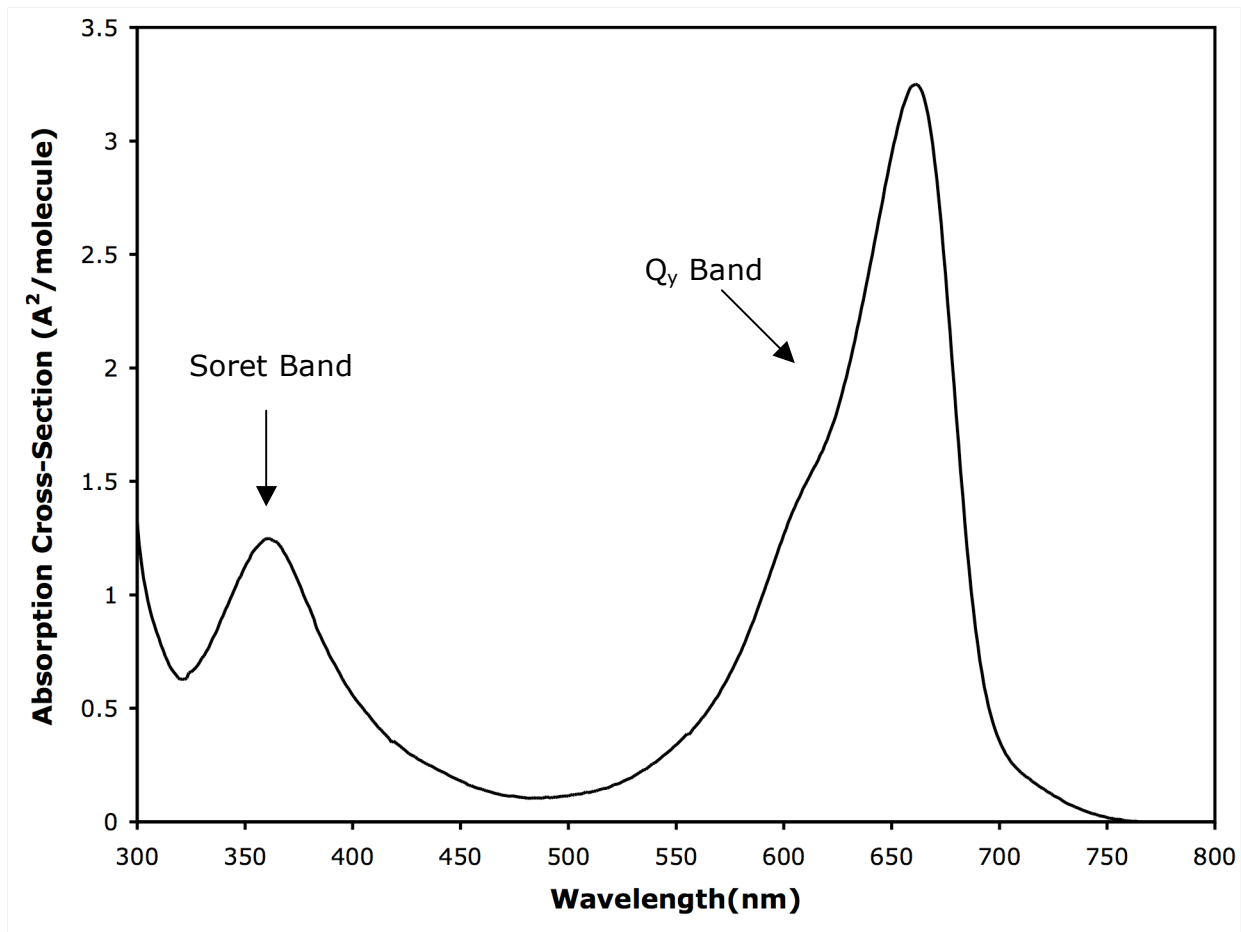


**Figure S1.** Experimental absorption spectrum of the P<sub>r</sub> form of phytochrome Cph1 at 295 K in glycerol-containing TES buffer. The band used in this analysis is the Q<sub>y</sub> band centered at 660 nm.

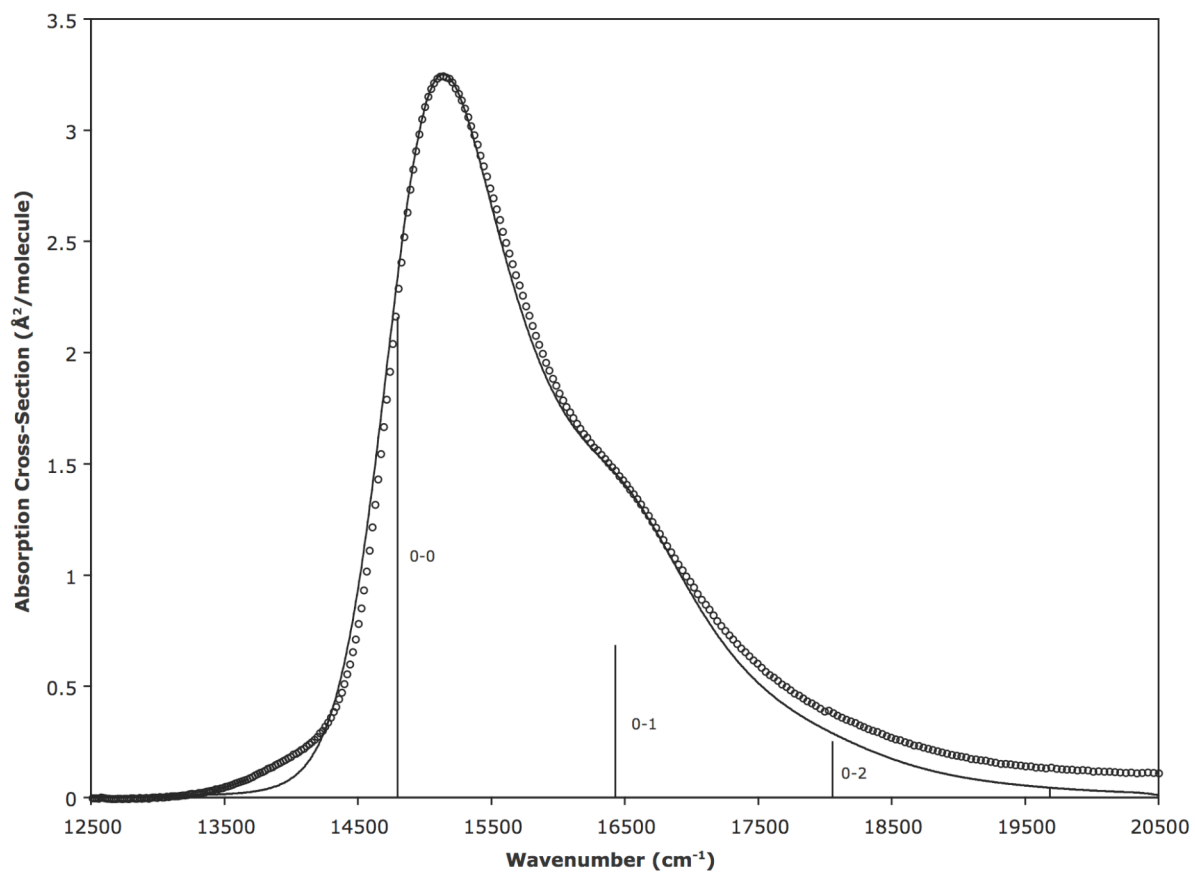


**Figure S2.** Experimental and calculated absorption spectra of the P<sub>r</sub> form of Cph1 at 295 K. The 0–0, 0–1, and 0–2 FC overlaps of the 1630 cm<sup>-1</sup> C=C stretch mode are shown.



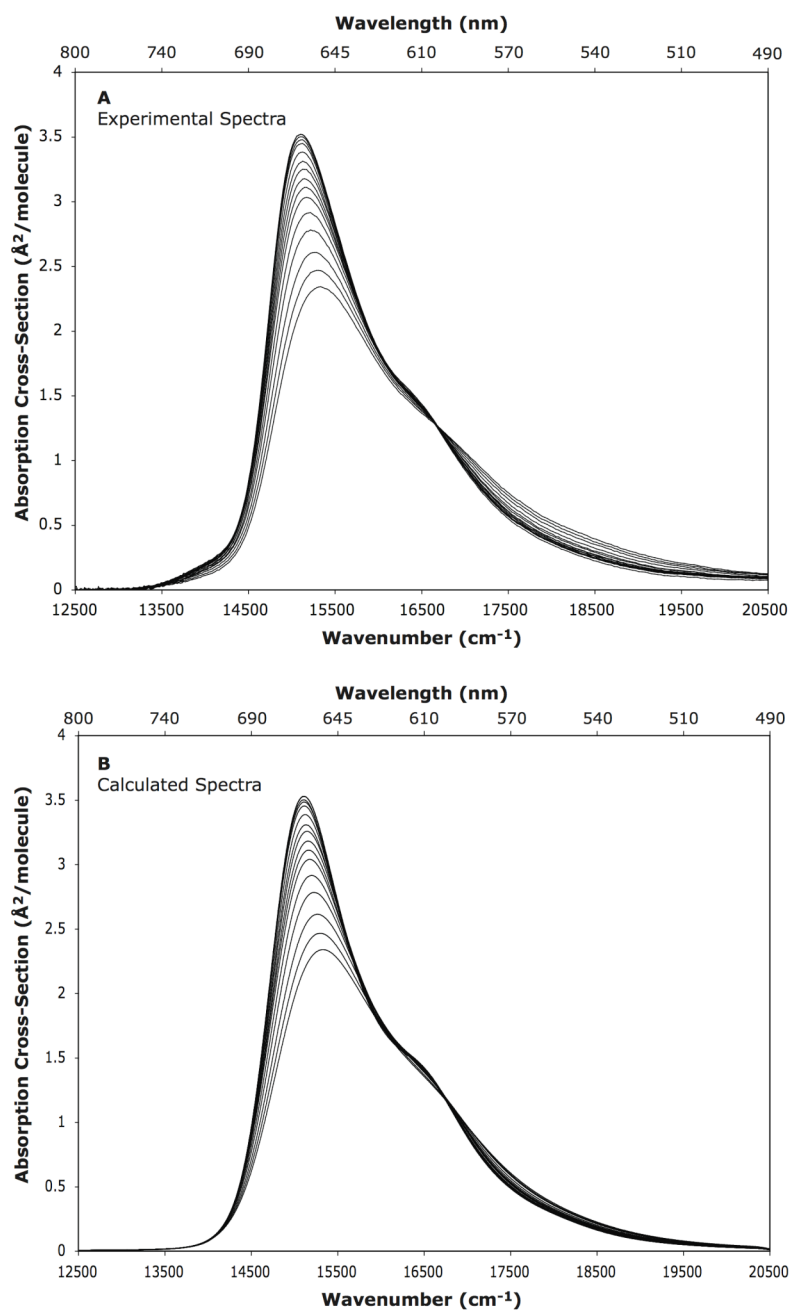


**Figure S3.** Comparison of the experimental (A) and calculated (B) absorption spectra of  $P_r$  at various temperatures between 281 and 313 K (8°C and 40°C). Note that the absorption cross-section decreases with increasing temperature. The experimental spectra show an isosbestic point at 600 nm, while the calculated spectra show an isosbestic point at 596 nm.

Temp. (K)	$\Gamma_G$ (cm <sup>-1</sup> )	M (Å)
281	820	2.34
282	820	2.33
283	825	2.35
286	830	2.34
288	835	2.33
291	850	2.33
294	865	2.32
296	880	2.32
298	895	2.31
300	905	2.29
302	920	2.28
304	945	2.26
306	975	2.24
309	1015	2.21
311	1045	2.18
313	1070	2.14

**Table S1.** Homogeneous broadening ( $\Gamma_G$ ) and electronic transition length (M) parameters over the range of temperatures used to calculate the spectra shown in Figure S3. For all plots, the 0–0 transition energy was 14800 cm<sup>-1</sup> and the inhomogeneous broadening was 90 cm<sup>-1</sup>.

#### S4. References

- (1) McCamant, D. W.; Kukura, P.; Yoon, S.; Mathies, R. A. *Rev. Sci. Instr.* **2004**, *75*, 4971-4980.
- (2) Myers, A. B.; Mathies, R. A. In *Biological Applications of Raman Spectroscopy. Resonance Raman Intensities: A Probe of Excited-State Structure and Dynamics*; Spiro, T. G., Ed.; John Wiley & Sons: New York, 1987; Vol. 2.
- (3) Dudik, J. M.; Johnson, C. R.; Asher, S. A. *J. Chem. Phys.* **1985**, *82*, 1732-1740.
- (4) Lee, S. Y.; Heller, E. J. *J. Chem. Phys.* **1979**, *71*, 4777-4788.
- (5) Tang, J.; Albrecht, A. C. In *Raman Spectroscopy*; Szymanski, H. A., Ed.; Plenum: New York, 1970; Vol.2.